Bias voltage dependence on the vibronic electric current

Tomomi Shimazaki and Yoshihiro Asai
National Institute of Advanced Industrial Science and Technology (AIST), Umezono, 1-1-1, Tsukuba Central 2, Tsukuba, Ibaraki 305-8568, Japan
and Core Research for Evolutional Science and Technology (CREST), Japan Science and Technology Corporation (JST), Kawaguchi 332-0012, Japan
(Received 2 October 2007; published 12 February 2008)

We discuss bias voltage effects on the elastic and the inelastic currents in the tunneling region. We have derived and solved two self-consistent loops: one for electron-electron interaction within the Hartree-Fock approximation, and another for the electron-intramolecular vibration coupling within the Born approximation. The formalism is based on Keldysh Green's function theory; numerical calculations were made in terms of *ab initio* quantum chemistry techniques augmented with a model for the electrodes. While no remarkable voltage effect on the vibronic currents was found in the low-bias voltage region, we found significant bias voltage effect in the high-bias voltage region. The suppressive correlation between the elastic and the inelastic components of the current is reduced because of the molecular orbital energy shift in the latter region.

DOI: 10.1103/PhysRevB.77.075110 PACS number(s): 73.63.−b, 72.10.−d, 68.37.Ef, 73.63.Rt

I. INTRODUCTION

The transport problem of single molecules bound between two electrodes (single molecular bridges) has become a matter of intense investigation.[1–3] The basic problem, which may bear serious importance at least partly due to the molecular electronics activity, however, is surely related to the electron transfer reaction studies in wet chemical environments that date back to early 1960s.[4] Although tunneling and hopping mechanisms were proposed more than a decade ago, the exponential decaying length dependent conductance[5,6] and the vibronic inelastic effects on the electric current in single molecular bridge systems[7–9] have received attention quite recently. Despite the large differences in the experimental setups required for these two problems, the problems themselves appear to be strongly correlated.[10] One benefit of the transport studies is that great precision is possible, both in theories and experiments, owing to the recent achievements in theoretical and experimental physics. The knowledge obtained in transport studies is important not only for the molecular electronics activity but also for solving basic problems in chemistry. Electron transfer reactions have wide application in important branches of chemistry, such as electrochemistry and biochemistry.

Inelastic tunneling spectroscopy (IETS) experiments have been applied to single molecules[11] and atomic wires.[12] Recent investigation has shown that the line shapes of d^2I/dV^2, i.e., the second derivative of the electric current taken against the bias voltage (V), as a function of V, for both these systems are quite different.[13] Here, electronic structure theories are modified to include the vibronic inelastic effect on the electric current. Theoretical calculations have become applicable for realistic single molecular bridges, atomic wires, and clusters at various levels of approximations of the electronic structure theory. The vibrational-mode assignments of IETS peaks have been made semiquantitatively. Besides these studies, investigations by Sergueev *et al.* address how a finite voltage effect modifies (or does not modify) the vibronic electric current.[14] First to study the problem, they found a strong bias voltage dependence of the dimensionless coupling constant λ for the electron-intramolecular vibration (e-mv) interaction. This problem needs be solved before further development of the electronic structure theory of the vibronic current is possible. Here, we study the bias voltage effects on the elastic and inelastic current in the tunneling region, where the gap between the Fermi level of the electrodes E_F and the site energy is larger than twice of the intramolecular transfer integral.[6] We used Keldysh Green's function theory combined with *ab initio* quantum chemistry techniques to study the bias voltage effect and the e-mv coupling effect. Here, however, we have adopted a simple tight-binding model for electrodes. The method, when it is applied to the former effect, is often called as the nonequilibrium Green's function (NEGF) method.[15–20] We adopt this notation for the bias voltage effect. The theory is applied to a hypothetical system where a benzenedithiolate molecule is suspended in the gap between the two electrodes. We have neglected nonequilibrium effects on molecular vibrations here, for simplicity. The effects may be expected to be small for molecules which have good thermal contact with electrodes.[21]

II. GENERAL THEORY

A. Keldysh Green's function formalism of electric current

In the following section, we present the formula for steady-state electric current through a single molecular bridge between two electrodes, in terms of the Keldysh Green's functions.[22] We denote the lesser Green's function of the center region, as shown in Fig. 1, by $G_C^<(\vec{r}_1,t_1;\vec{r}_2,t_2)$. This will be described later, but it includes the contact effect between the molecule and the electrodes, the electron-electron interaction in the molecule, and the e-mv coupling effect. The zeroth order lesser Green's function is given by $G_C^{(0)<}(\vec{r}_1,t_1;\vec{r}_2,t_2) \equiv i\langle \Psi^\dagger(\vec{r}_1,t_1)\Psi(\vec{r}_2,t_2)\rangle$, where $\Psi^\dagger$ (Ψ) is the field creation (annihilation) operator, and $\vec{r}$ and t denote the position vector and time variable of an electron; a nu-

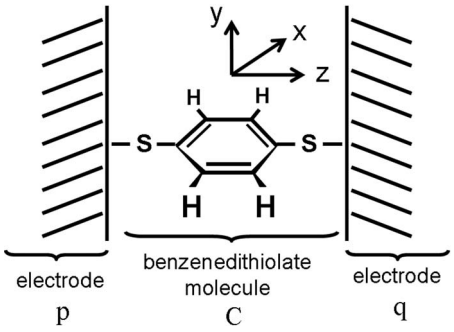

FIG. 1. Benzenedithiolate molecule and model electrodes. The z axis is aligned such that it goes through the sulfur atoms of the molecule, and the x axis is lying on the molecular plane.

meric subscript is the label for the electron. The total number of electrons in the molecule is given by $n_e(t) = 1/2\pi i \int_{molecule} G_C^<(r,t;r,0)d\vec{r}$, where the space integral is taken over the molecular region. The electric current through the single molecular bridge is defined by $j(t) \equiv -2e(d/dt)n_e(t)$, where factor 2 comes from spins. If we use the equation of motion for the lesser Green's function, the microcanonical electric current $j(E) \equiv \int j(t)e^{iEt}dt$ is then given by

$$j(E) = -2\frac{e}{2\pi i}\int_{molecule}\frac{d}{dt}G_C^<(\vec{r},\vec{r};E)d\vec{r}$$
$$= -\frac{2e}{h}\int_{molecule}[H_C G_C^<(\vec{r},\vec{r}';E) - G_C^<(\vec{r},\vec{r}';E)H_C]_{\vec{r}=\vec{r}'}d\vec{r}, \tag{1}$$

where $G_C^<(\vec{r},\vec{r}';E) = \int G_C^<(\vec{r},t;\vec{r}',0)e^{iEt}dt$ and H_C is the Hamiltonian of the center region, which satisfies the relation[23]

$$(E + i\eta - H_C)G_C^R(\vec{r}_1,\vec{r}_2;E) - \int d\vec{r}_3\Sigma_C^R(\vec{r}_1,\vec{r}_3;E)G_C^R(\vec{r}_3,\vec{r}_2;E)$$
$$= \delta(\vec{r}_1 - \vec{r}_2), \tag{2a}$$

where $G_C^R(\vec{r}_1,\vec{r}_2;E)$ is the retarded Green's function of the center region, and $\Sigma_C^R(\vec{r}_1,\vec{r}_3;E)$ is the sum of the self-energies due to the contact between the molecule and electrodes, the electron-electron interaction in the molecule, and the e-mv coupling, which will be described subsequently. E is the energy and η is an infinitesimal positive constant. The corresponding self-adjoint relation

$$G_C^A(\vec{r}_1,\vec{r}_2;E)(E - i\eta - H_C) - \int d\vec{r}_3 G_C^A(\vec{r}_1,\vec{r}_3;E)\Sigma_C^A(\vec{r}_3,\vec{r}_2;E)$$
$$= \delta(\vec{r}_1 - \vec{r}_2) \tag{2b}$$

is also satisfied by H_C. By using these equations, the steady-state kinetic equations[23]

$$G_C^<(\vec{r},\vec{r}';E) = \int\int G_C^R(\vec{r},\vec{r}_1;E)\Sigma_C^<(\vec{r}_1,\vec{r}_2;E)G_C^A(\vec{r}_2,\vec{r}';E)d\vec{r}_1 d\vec{r}_2, \tag{3a}$$

$$G_C^>(\vec{r},\vec{r}';E) = \int\int G_C^R(\vec{r},\vec{r}_1;E)\Sigma_C^>(\vec{r}_1,\vec{r}_2;E)G_C^A(\vec{r}_2,\vec{r}';E)d\vec{r}_1 d\vec{r}_2, \tag{3b}$$

and the identity relation $\Sigma_C^> - \Sigma_C^< = \Sigma_C^R - \Sigma_C^A$, the formula of the energy dependent electric current is obtained[23] as follows:

$$j(E) = \frac{2e}{h}\int\int_{molecule}[\Sigma_C^>(\vec{r}_1,\vec{r}_2;E)G_C^<(\vec{r}_2,\vec{r}_1;E)$$
$$- \Sigma_C^<(\vec{r}_1,\vec{r}_2;E)G_C^>(\vec{r}_2,\vec{r}_1;E)]d\vec{r}_1 d\vec{r}_2, \tag{4}$$

where $\Sigma_C^<$ and $\Sigma_C^>$ are the lesser and the greater self-energies. The remaining problem is to calculate the self-energies which are also necessary to calculate the lesser and greater Green's functions. This will be addressed in the following subsections.

B. Self-energy due to contact between the molecule and the electrodes

The self-energy $\Sigma_C^R(\vec{r}_1,\vec{r}_2;E)$ is given by the sum of the following three contributions:

$$\Sigma_C^R(\vec{r}_1,\vec{r}_2;E) = \Sigma_{contact}^R(\vec{r}_1,\vec{r}_2;E) + \Sigma_{e\text{-}e}^R(\vec{r}_1,\vec{r}_2;E)$$
$$+ \Sigma_{e\text{-}mv}^R(\vec{r}_1,\vec{r}_2;E), \tag{5}$$

where the first, second, and third terms on the right-hand side of the equation denote the retarded self-energies due to the contact effect, the electron-electron interaction effect, and the e-mv coupling effect, respectively. We use the atomic orbital basis $\chi_\alpha(\vec{r})$ to express the matrix element of the Hamiltonian, the overlap, Green's function, and the self-energies for the molecule and electrodes, as well as the coupling between them, i.e., $H_{\alpha\beta} = \langle\chi_\alpha(\vec{r})|H(r)|\chi_\beta(\vec{r})\rangle$, $S_{\alpha\beta} = \langle\chi_\alpha(\vec{r})|\chi_\beta(\vec{r})\rangle$, $G^R(\vec{r}_1,\vec{r}_2;E) = \Sigma_{\alpha,\beta}\chi_\alpha(\vec{r}_1)G_{\alpha\beta}^R(E)\chi_\beta(\vec{r}_2)$, and $\Sigma_{\alpha\beta}^R(E) = \langle\chi_\alpha(\vec{r}_1)|\Sigma_C^R(\vec{r}_1,\vec{r}_2;E)|\chi_\beta(\vec{r}_2)\rangle$, respectively. The one-electron Hamiltonian is given by

$$H(\vec{r}) = -\frac{1}{2}\frac{\partial^2}{\partial\vec{r}^2} - \sum_A\frac{Z_A e^2}{|\vec{r} - \vec{R}_A|}, \tag{6a}$$

where Z_A is the atomic number of nucleus A, and $\vec{R}_A$ denotes its position vector. The total electronic Hamiltonian is simply given by

$$H_{\text{total}} = \sum_i H(\vec{r}_i) + \sum_{i<j}\frac{e^2}{|\vec{r}_i - \vec{r}_j|}, \tag{6b}$$

where the second term in the right-hand side of Eq. (6b) denotes the electron-electron repulsions. In this paper, the

many-body effects due to electron-electron repulsions are approximated in terms of the Hartree-Fock self-energy, which will be discussed later. For the moment, we will discuss the problem in terms of noninteracting Hamiltonian. The retarded Green's function of system $\mathbf{G}^R=[(E+i\eta)\mathbf{S}-\mathbf{H}]^{-1}$, which consists of the molecule and the semi-infinite electrodes, is described by the Hamiltonian and overlap matrices decomposed into submatrices as

$$\mathbf{H}=\begin{pmatrix} \mathbf{H}_p & \mathbf{H}_{p,C} & \mathbf{0} \\ \mathbf{H}_{p,C}^T & \mathbf{H}_C & \mathbf{H}_{q,C}^T \\ \mathbf{0} & \mathbf{H}_{q,C} & \mathbf{H}_q \end{pmatrix}, \tag{7a}$$

$$\mathbf{S}=\begin{pmatrix} \mathbf{S}_p & \mathbf{S}_{p,C} & \mathbf{0} \\ \mathbf{S}_{p,C}^T & \mathbf{S}_C & \mathbf{S}_{q,C}^T \\ \mathbf{0} & \mathbf{S}_{q,C} & \mathbf{S}_q \end{pmatrix}, \tag{7b}$$

where $\mathbf{H}_C$ is the Hamiltonian submatrix of the molecule, and $\mathbf{H}_{p(q)}$ denotes that of the semi-infinite electrode labeled as $p(q)$, shown in Fig. 1. $\mathbf{S}_C$ is the overlap submatrix of the molecule and $\mathbf{S}_{p(q)}$ denotes that of the semi-infinite electrodes labeled as $p(q)$. $\mathbf{H}_{C,p(q)}$ denotes the off-diagonal submatrix of the Hamiltonian, which expresses the coupling between the molecule and the semi-infinite electrode $p(q)$. $\mathbf{S}_{C,p(q)}$ denotes the off-diagonal submatrix of the overlap between the molecule and the semi-infinite electrode $p(q)$. However, there are no off-diagonal matrix elements between the electrodes p and q, for either the Hamiltonian or the overlap; that is, there are no direct interactions between the electrodes. Because of the semi-infiniteness of the electrodes, the matrix dimension of Green's function for system $\mathbf{G}^R$ is infinite, and is therefore difficult to handle. This problem has been solved by introducing the following retarded self-energy of interaction between the molecule and electrode $p(q)$.

$$\mathbf{\Sigma}_{p(q)}^R=\boldsymbol{\tau}_{p(q),C}^T\mathbf{G}_{p(q)}^R\boldsymbol{\tau}_{p(q),C}, \tag{8}$$

where $\mathbf{G}_{p(q)}^R=[(E+i\eta)\mathbf{S}_{p(q)}-\mathbf{H}_{p(q)}]^{-1}$, and $\boldsymbol{\tau}_{p(q),C}=\mathbf{H}_{p(q),C}-E\mathbf{S}_{p(q),C}$.[23] We usually use truncations for the range of the coupling matrix $\boldsymbol{\tau}_{p(q),C}$ between the molecule and the electrode because it is expected to decrease very rapidly inside the electrode. The retarded Green's function of the center region, $\mathbf{G}_C^R$, which includes interactions between the molecule and the electrodes is obtained from the above self-energy, as follows:

$$\mathbf{G}_C^R=[(E+i\eta)\mathbf{S}_C-\mathbf{H}_C-\mathbf{\Sigma}_p^R-\mathbf{\Sigma}_q^R]^{-1}. \tag{9}$$

While the dimension of $\mathbf{G}_C^R$ is finite, the semi-infinite nature of the electrodes is included here through the self-energy.[23]

We may suppose that thermal equilibrium is achieved for electrons in the electrode, and may impose the following boundary condition on the time variable of the contact self-energy $\mathbf{\Sigma}_{contact}^<(t_1,t_2)\equiv\mathbf{\Sigma}_p^<(t_1,t_2)+\mathbf{\Sigma}_q^<(t_1,t_2)$:

$$\mathbf{\Sigma}_{p(q)}^<(t_1=0,t_2)=-e^{\beta\mu_{p(q)}}\mathbf{\Sigma}_{p(q)}^>(t_1=-i\beta,t_2), \tag{10}$$

where $\mu_{p(q)}$ is the chemical potential of the electrode $p(q)$ and $\beta=1/k_BT$ is the inverse of the temperature, multiplied by the Boltzmann constant k_B.[24] The chemical potential $\mu_{p(q)}$ may be determined by the voltage V, in terms of $\mu_{p(q)}=E_F+\zeta_{p(q)}V$, where E_F is the Fermi level of the electrodes, and $\zeta_{p(q)}$ represents the voltage division factors that satisfy $\zeta_q-\zeta_p=1$, i.e., $\mu_q-\mu_p=V$. In this paper, we have supposed that two electrodes are identical and have followed arguments for the voltage division factor of symmetric electrodes found in literatures.[18,25] Thus, we have set $\zeta_q=0.5$. It should be noted that the molecule and the coupling between the molecule and the electrode have to be symmetric in our case, because we have put the boundary between the center region and its outside on the link between the terminal atoms of the molecule and the outmost atom of the electrode. The chemical potentials at the boundaries give the boundary conditions for the NEGF self-consistent field (SCF), and the electrostatic potential and the level alignments within the center region are self-consistently determined under the boundary conditions. If we use the Fourier transform for the time variable, and the identity relation $\mathbf{\Sigma}_{p(q)}^>-\mathbf{\Sigma}_{p(q)}^<=\mathbf{\Sigma}_{p(q)}^R-\mathbf{\Sigma}_{p(q)}^A$, we obtain the following expression for the lesser and greater self-energies of the thermalized electrodes:

$$-i\mathbf{\Sigma}_{p(q)}^<(E)=if_{p(q)}(E)[\mathbf{\Sigma}_{p(q)}^R(E)-\mathbf{\Sigma}_{p(q)}^A(E)], \tag{11a}$$

$$i\mathbf{\Sigma}_{p(q)}^>(E)=i[1-f_{p(q)}(E)][\mathbf{\Sigma}_{p(q)}^R(E)-\mathbf{\Sigma}_{p(q)}^A(E)], \tag{11b}$$

where $f_{p(q)}(E)=1/[e^{\beta(E-\mu_{p(q)})}+1]$ is the Fermi-Dirac distribution function for the electrode $p(q)$. The corresponding matrix representation of these self-energies may be obtained likewise. Note that finally the formula of the energy resolved electric current in the matrix notation should be read as[23]

$$j(E)=\frac{2e}{h}\mathrm{Tr}[\mathbf{\Sigma}_C^>(E)\mathbf{G}_C^<(E)-\mathbf{\Sigma}_C^<(E)\mathbf{G}_C^>(E)]. \tag{12}$$

The total electric current is then given by

$$I=I_p+I_q=\frac{2e}{h}\int_{-\infty}^{+\infty}\mathrm{Tr}[\mathbf{\Sigma}_C^>(E)\mathbf{G}_C^<(E)-\mathbf{\Sigma}_C^<(E)\mathbf{G}_C^>(E)]dE, \tag{13}$$

where $I_{p(q)}$ is the terminal current of the electrode $p(q)$. The trace appears in Eq. (13) because the current in this atomic orbital representation is written by $j(t)=-2(e/2\pi i)(d/dt)\mathrm{Tr}[\mathbf{G}_C^<]$ rather than that in the coordinate representation given in Eq. (4).

C. Hartree-Fock self-energy for electron-electron interactions

Here, we derive the equation for self-energy due to electron-electron interaction $\mathbf{\Sigma}_{e\text{-}e}^R(E)$. The chronological self-energy for the interaction in the Haretree-Fock approximation is given by[26,27]

$$[\mathbf{\Sigma}^t_{HF}(t_1,t_2)]_{\alpha\beta} = -i\delta(t_1-t_2)\sum_{\gamma\zeta}\langle\alpha\gamma||\beta\zeta\rangle G^t_{C;\gamma\zeta}(t_1,t_1^+)$$
$$= -i\delta(t_1-t_2)\sum_{\gamma\zeta}\langle\alpha\gamma||\beta\zeta\rangle G^<_{C;\gamma\zeta}(t_1,t_1^+), \quad (14)$$

where Greek letters denote the suffixes for atomic orbital basis functions. $t_1^+ \equiv t_1+\eta$, where η is the infinitesimal positive constant. The chronological, noninteracting Green's function is defined in terms of the time-ordering operator T_t; $G^t(\vec{r}_1,t_1;\vec{r}_2,t_2) \equiv -i\langle T_t[\Psi(\vec{r}_1,t_1)\Psi^\dagger(\vec{r}_2,t_2)]\rangle$. The corresponding matrix element, $G^t_{C;\gamma\zeta}(t_1,t_2)$, is calculated using the relation $G^t_C(\vec{r}_1,t_1;\vec{r}_2,t_2) = \Sigma_{\gamma,\zeta}\chi_\gamma(\vec{r}_1)G^t_{C;\gamma\zeta}(t_1,t_2)\chi_\zeta(\vec{r}_2)$. We use similar notation for matrix elements of other Green's functions, i.e., $G^{>(<)}_C(\vec{r}_1,t_1;\vec{r}_2,t_2) = \Sigma_{\gamma,\zeta}\chi_\gamma(\vec{r}_1)G^{>(<)}_{C;\gamma\zeta}(t_1,t_2)\chi_\zeta(\vec{r}_2)$ and $G^{R(A)}_C(\vec{r}_1,t_1;\vec{r}_2,t_2) = \Sigma_{\gamma,\zeta}\chi_\gamma(\vec{r}_1)G^{R(A)}_{C;\gamma\zeta}(t_1,t_2)\chi_\zeta(\vec{r}_2)$. $\langle\alpha\gamma||\beta\zeta\rangle$ is given in terms of the two-electron integrals

$$\langle\alpha\gamma||\beta\zeta\rangle = 2\langle\alpha\gamma|\beta\zeta\rangle - \langle\alpha\gamma|\zeta\beta\rangle, \quad (15)$$

where we have used the standard notation used in quantum chemistry books.[28]

$$\langle\alpha\gamma|\beta\zeta\rangle = \int \chi_a(\vec{r}_1)\chi_\gamma(\vec{r}_2)\frac{1}{|\vec{r}_1-\vec{r}_2|}\chi_\beta(\vec{r}_1)\chi_\zeta(\vec{r}_2)dr_1dr_2. \quad (16)$$

Note that the definition of the chronological Green's function $\mathbf{G}^t_C(t_1,t_2) = \theta(t_1-t_2)\mathbf{G}^>_C(t_1,t_2) + \theta(t_2-t_1)\mathbf{G}^<_C(t_1,t_2)$ has been used to arrive at the final expression in Eq. (14).[22] The Hartree-Fock self-energy is then given in terms of the density matrix, whose element is given by $P_{\gamma\zeta} \equiv 1/2\pi i\int_{-\infty}^{\infty}G^<_{C;\gamma\zeta}(E)dE$;

$$[\mathbf{\Sigma}^t_{HF}(t_1,t_2)]_{\alpha\beta} = \delta(t_1-t_2)\sum_{\gamma\zeta}\langle\alpha\gamma||\beta\zeta\rangle\frac{1}{2\pi i}\int_{-\infty}^{\infty}G^<_{C;\gamma\zeta}(E)dE$$
$$= \delta(t_1-t_2)\sum_{\gamma\zeta}\langle\alpha\gamma||\beta\zeta\rangle P_{\gamma\zeta}, \quad (17a)$$

where we have used $\mathbf{G}^<_C(t_1,t_2) = 1/2\pi\int_{-\infty}^{\infty}e^{-iE(t_1-t_2)}\mathbf{G}^<_C(E)dE$. Similarly,

$$[\mathbf{\Sigma}^t_{HF}(E)]_{\alpha\beta} = \int_{-\infty}^{\infty}e^{iEt}[\mathbf{\Sigma}^t_{HF}(t)]_{\alpha\beta}dt$$
$$= \int_{-\infty}^{\infty}e^{iEt}\delta(t)\sum_{\gamma\zeta}\langle\alpha\gamma||\beta\zeta\rangle P_{\gamma\zeta}dt$$
$$= \sum_{\gamma\zeta}\langle\alpha\gamma||\beta\zeta\rangle P_{\gamma\zeta}. \quad (17b)$$

It should be noted that the chronological self-energy $\mathbf{\Sigma}^t_{HF}$ does not have energy dependence. Its time dependence is described exclusively by the delta function. In general, $\mathbf{\Sigma}^t(t) = \mathbf{\Sigma}^\delta\delta(t) + \theta(t)\mathbf{\Sigma}^>(t) + \theta(-t)\mathbf{\Sigma}^<(t)$, therefore it is clear that $\mathbf{\Sigma}^{<(>)}_{HF}=0$. Because $\mathbf{\Sigma}^{R(A)}_{HF} = \mathbf{\Sigma}^t_{HF} - \mathbf{\Sigma}^{<(>)}_{HF} = \mathbf{\Sigma}^t_{HF}$ is purely real, the real value does not change whether it is the retarded or advanced self-energy. Standard quantum chemical techniques can be used to calculate $\mathbf{\Sigma}^{R(A)}_{HF}$.

Boundary conditions must be imposed at the interface between the molecule and the electrodes not only for the wave function and the Green's function but also for the electrostatic potential function ϕ. The electrostatic potential function at the molecular edge must be coincident with that of the electrode, which is linked to the molecular edge. Then the molecule is exposed to the potential gradient (electric field) given by $(\phi_p-\phi_q)/L$, where L is the length of the molecule and $\phi_{p(q)}$ is the electrostatic potential function at the electrode $p(q)$. If the electrodes are identical, the potential difference is given in terms of the applied voltage difference V between the electrodes, i.e., $\phi_p-\phi_q=V$. Thus, the electric field, which is applied along the molecular axis, is given by V/L. The field gradient term must be included in the extended molecule calculation when $V\neq 0$.[17,29] The matrix element of the field gradient term is given by $[\mathbf{\Xi}]_{\alpha\beta} = -\vec{E}\cdot\langle x_\alpha|\vec{r}|x_\beta\rangle$. $\vec{E}$ is the electronic field determined by the boundary condition for the potential function, and is given by $\vec{E}=\vec{\mathbf{e}}_z V/L$. $\vec{\mathbf{e}}_z$ is the unit vector for the z direction, and the molecular axis should align in the z direction, shown in Fig. 1. We put the origin of the coordinate on the center of the benzendithiolate molecule, so the surfaces of electrodes p and q are located at $z=-0.5L$ and $z=0.5L$, respectively. More details of the discussions related to the field gradient term and the electrostatic potential are found in Ref. 20.

We frequently use the Hartree-Fock Hamiltonian matrix $\mathbf{F}$, rather than the original Hamiltonian matrix $\mathbf{H}_C$, i.e., $\mathbf{F} \equiv \mathbf{H}_C + \mathbf{\Sigma}^{R(A)}_{HF} + \mathbf{\Xi}$ as it includes the field gradient term. The most important consequence here is that, because $\mathbf{\Sigma}^{<(>)}_{HF}=0$, electron-electron interaction effects do not play any dynamic role in the kinetic equation,[15,18] but they do play a static role in modulating the potential inside the center region through $P_{\gamma\zeta} \equiv 1/2\pi i\int_{-\infty}^{\infty}G^<_{\gamma\zeta}(E)dE$, which gives rise to voltage-dependent occupations of electrons over the molecular orbitals. Green's function theories applied to the electron-electron interaction problem within the mean-field approximations, i.e., the Hartree-Fock approximation and the local density approximation (LDA), are often referred to as the NEGF method. We follow this notation. The LDA approach, however, derives no clear proof to show $\mathbf{\Sigma}^{<(>)}_{LDA}=0$; thus an ambiguity remains in the fundamental basis of the LDA-based NEGF theory.

While the Hartree-Fock approximation overestimates the energy gap between the highest occupied molecular orbital (HOMO) and the lowest unoccupied molecular orbital (LUMO) of molecules, the LDA underestimates the HOMO-LUMO gap. By using some of the conserving approximations,[24] such like the random phase approximation, T-matrix approximation, for example, it may be possible to take into account of weak electronic correlation effects beyond the Hartree-Fock approximation and the LDA. The conserving approximations, which are not very accurate, may be useful to correct some of the errors in the Hartree-Fock approximation and the LDA but not all of them. Some of the sophisticated theories useful for equilibrium systems do not satisfy the conservation law and hence it is not safe to use them for the transport problem. Clearly, the accuracy problem remains in the transport theory as far as the electron-electron interaction is concerned. The problem has

been thought to be one of the possible sources of the discrepancy between the experimental electric current value and their theoretical values whose ratio may be 10^2 or larger.

D. Total energy and the molecular vibrations

The total energy problem in our open bridge junction systems is a difficult but well known problem.[30,31] It seems that the full problem is still to be resolved. A treatise often adopted in literatures is to use the total energy formula of the isolated molecule or the extended molecule in the center region for the calculation of the total energy of the open bridge junction system. The trick used there is to substitute the energy integrated lesser Green's function of the open bridge junction system $1/2\pi i\int_{-\infty}^{\infty} G_{\gamma\zeta}^{<}(E)dE$ into the density matrix terms $P_{\gamma\zeta}$ in the total energy formula.[31] By doing that, nonequilibrium effect for electrons in the open bridge junction system is partly taken into account. The contact self-energy effect has not been taken into account in the total energy formula, explicitly however.

In this approximation, the bias voltage-dependent total energy is determined as follows:

$$E_{HF}(V) = \sum_{\alpha,\beta} P_{\alpha\beta}(V)F_{\alpha\beta} - \frac{1}{2}\sum_{\alpha,\beta} P_{\alpha\beta}(V)P_{\delta\gamma}(V)\langle\alpha\beta||\gamma\delta\rangle + V_{nn} + V_{n\text{-}field}, \quad (18)$$

where $F_{\alpha\beta}$ is the matrix element of the Fock matrix, V_{nn} is the nucleus-nucleus repulsive energy, and $V_{n\text{-}field}$ is the interaction energy between nuclei and the external electric field. The Hartree-Fock total energy $E_{HF}(V)$ depends on the applied bias voltage through the density matrix contributions $\mathbf{P}(V)$, which is calculated from Eqs. (31a) and (31b). A part of the scattering state effects is taken into account through the NEGF-based density matrix discussed in Sec. III. The bias-dependent Hessian matrix and, hence, the normal vibrations of the molecule are calculated from the second derivative of the $E_{HF}(V)$ with respect to the nuclear coordinates.

E. Electron-intramolecular vibration self-energy

In order to discuss the molecular vibration effect on the electric current, we expand the molecular orbital energy parts ε_a of the Hartree-Fock single particle Hamiltonian $\hat{F} = \Sigma_a \varepsilon_a \hat{c}_a^{\dagger}\hat{c}_a$ in terms of the normal coordinate q of the molecular vibration: $\varepsilon_a \simeq \varepsilon_a(0) + (\partial\varepsilon_a/\partial q)(0)\cdot q$. The linear term of $\hat{F}$ with respect to q gives perturbation Hamiltonian of our e-mv problem. Most standard treatise that derive the lesser and the greater self-energies is to use the Langreth theorem[32] for chronological self-energies in the time domain. If we use the lowest-order perturbation theory for the contact self-energy which will be discussed in the Sec. III A and Appendix B, the lowest-order chronological self-energy for e-mv coupling may be given by[22]

$$\Sigma_{e\text{-}mv}^{t}(t,t') = \frac{i}{2\pi}\sum_{s} \kappa^s D_s^t(t,t')G_C{}^t(t,t'), \quad (19)$$

where the suffix s classifies the normal vibrational mode, κ^s is the squared e-mv coupling constant which will be given by Eq. (34) in Sec. III A, and $D_s^t(t,t')$ is the chronological Green's function of the molecular vibration, whose Fourier transform onto the energy domain is given by

$$D_s^t(\omega) = \frac{1}{\omega - \omega_s + i\delta\,\mathrm{sgn}(\omega)} - \frac{1}{\omega + \omega_s + i\delta\,\mathrm{sgn}(\omega)}. \quad (20)$$

Because of the Langreth theorem, the product of the chronological Green's function for the electron and the vibration $D_s^t(t,t')G_C^t(t,t')$ may give rise to those of the lesser and greater Green's function, $D_s^<(t,t')G_C^<(t,t')$ and $D_s^>(t,t')G_C^>(t,t')$, respectively.[32] Using the theorem, we may obtain the following lesser and greater self-energies of e-mv origin:

$$\Sigma_{e\text{-}mv}^{<}(E) = \frac{i}{2\pi}\sum_{s} \kappa^s \int d\omega D_s^<(\omega)G_C^<(E-\omega), \quad (21a)$$

$$\Sigma_{e\text{-}mv}^{>}(E) = \frac{i}{2\pi}\sum_{s} \kappa^s \int d\omega D_s^>(\omega)G_C^>(E-\omega), \quad (21b)$$

we may suppose that the molecular vibration is in thermal equilibrium, and therefore we impose the following boundary condition for the time variable of the lesser Green's function of the vibration:

$$D_{p(q)}^<(\vec{r}_1,\vec{r}_2;t_1=0,t_2) = D_{p(q)}^>(\vec{r}_1,\vec{r}_2;t_1=-i\beta,t_2). \quad (22)$$

This leads to the following relation between the lesser and the greater Green's function:

$$D_{p(q)}^<(\vec{r}_1,\vec{r}_2;\omega) = e^{-\beta\omega}D_{p(q)}^>(\vec{r}_1,\vec{r}_2;\omega). \quad (23)$$

The spectrum function representation of the e-mv self-energies is then given as

$$\Sigma_{e\text{-}mv}^{<}(E) = \frac{i}{2\pi}\sum_{s} \int \kappa^s J_s(\omega)G_C{}^<(E-\omega)d\omega, \quad (24a)$$

$$\Sigma_{e\text{-}mv}^{>}(E) = \frac{i}{2\pi}\sum_{s} \int \kappa^s J_s(\omega)G_C{}^>(E+\omega)d\omega. \quad (24b)$$

The vibrational spectral function $J_s(\omega)$ is given by

$$J_s(\omega) = b(\omega_s)\delta(\omega-\omega_s) + \{1+b(\omega_s)\}\delta(\omega+\omega_s), \quad (25)$$

where ω_s denotes the vibrational frequency of the normal mode s and the Bose distribution function is given by $b(|\omega|) = 1/[e^{\beta|\omega|}-1]$. Damping effects and the local heating problem on the molecular vibration cause complications and therefore they will not be discussed here.

F. Self-consistent theory

The previous subsections derived the self-energies due to contact, electron-electron interaction, and e-mv coupling. While the steady-state kinetic equations, Eqs. (3a) and (3b), that give the lesser and greater Green's function include the lesser and greater self-energies as inputs, the self-energies are calculated in terms of Green's function, shown in Eqs. (21a) and (21b). We therefore need self-consistent calcula-

tions to determine both. However, this is true only for the e-mv coupling contribution, and different for the contact interaction. We do not need a self-consistent calculation to determine the contact contribution to the self-energies, because the interaction is accurately solved using Eq. (11b). No kinetic equations need to be solved for contact self-energies. For electron-electron interaction, however, we do need self-consistent calculations to determine $\mathbf{\Sigma}_{HF}^{R(A)}$, despite $\mathbf{\Sigma}_{HF}^{<(>)}=0$. Because of this relation, there are no contributions from the electron-electron interactions to the kinetic equation, but $\mathbf{\Sigma}_{HF}^{R(A)}$ must be consistent with $\mathbf{G}_C^{R(A)}$. While $\mathbf{\Sigma}_{HF}^{R(A)}$ is given by $\mathbf{G}_C^{R(A)}$ because of Eq. (19) and the relation

$$\mathbf{P} = \frac{1}{2\pi i}\int_{-\infty}^{\infty} \mathbf{G}_C^{<}(E)dE$$

$$= \frac{1}{2\pi}\int_{-\infty}^{\infty} [f_p(E)\mathbf{G}_C^R\mathbf{\Gamma}_p\mathbf{G}_C^A + f_q(E)\mathbf{G}_C^R\mathbf{\Gamma}_p\mathbf{G}_C^A - i\mathbf{G}_C^R\mathbf{\Sigma}_{e\text{-}mv}^{<}\mathbf{G}_C^A]dE, \quad (26)$$

where $\mathbf{\Gamma}_{p(q)}(E)=i(\mathbf{\Sigma}_{p(q)}^R-\mathbf{\Sigma}_{p(q)}^A)$, and $\mathbf{G}_C^{R(A)}$ is dependent on $\mathbf{\Sigma}_C^{R(A)}$, which includes $\mathbf{\Sigma}_{HF}^{R(A)}$ instead of $\mathbf{\Sigma}_{e\text{-}e}^{R(A)}$ in Eq. (5). We therefore need to determine another self-consistent quantity. We need two loops to get self-consistencies, one for e-mv coupling and another for electron-electron interaction. Because of the last term in Eq. (26), $-i\mathbf{G}_C^R\mathbf{\Sigma}_{e\text{-}mv}^{<}\mathbf{G}_C^A$, the two loops are not independent. Nonetheless, we will separate the loops for numerical calculations, which will be presented later. If $\mathbf{\Sigma}_{e\text{-}mv}^{<}$ is small compared with $\mathbf{\Gamma}_{p(q)}$, which is expected for molecules, this simplification may not change our numerical results; however, it reduced the computational cost significantly, and it is useful practically. Because of the contact effect, both $\mathbf{\Sigma}_{HF}^{R(A)}$ and $\mathbf{G}_C^{R(A)}$ are dependent on the voltage.

III. IMPLEMENTATION THEORIES

A. Approximate Green's functions

This section derives a practical theory, which will enable further simplifications. In the previous section, we used the direct inverse of a Hamiltonian based matrix to calculate the retarded and advanced Green's functions. Here, we use the Lehmann representation of Green's function, in terms of the molecular orbitals, with some modification.[29] The retarded Green's function may be given in terms of molecular orbital coefficient vectors, $\mathbf{C}_a^R$ and $\mathbf{C}_a^A$, of molecular orbitals of the center region, defined on the dual space $\{\varphi_a(\vec{r})\}$ and $\{\psi_a(\vec{r})\}$ as follows:

$$\mathbf{G}_C^R = \sum_a^M \frac{\mathbf{C}_a^R\mathbf{C}_a^{A\dagger}}{E-\varepsilon_a}, \quad (27a)$$

$$[\mathbf{F}+\mathbf{\Sigma}_{contact}^R+\mathbf{\Sigma}_{e\text{-}mv}^R]\mathbf{C}_a^R = \varepsilon_a\mathbf{S}\mathbf{C}_a^R, \quad (27b)$$

$$[\mathbf{F}+\mathbf{\Sigma}_{contact}^A+\mathbf{\Sigma}_{e\text{-}mv}^A]\mathbf{C}_a^A = \varepsilon_a^*\mathbf{S}\mathbf{C}_a^A, \quad (27c)$$

where the molecular orbital coefficient vectors are given by eigenvectors of dual Schrödinger equations, Eqs. (27b) and (27c), for our open system. The subscript a is the molecular orbital index. We use relations, i.e., $G_C^R(r_1,r_2;E)=\Sigma_a\frac{\varphi_a(r_1)\psi_a^*(r_2)}{E-\varepsilon_a}$, $G_C^R(\vec{r}_1,t_1;\vec{r}_2,t_2)=\Sigma_{\gamma,\zeta}\chi_\gamma(\vec{r}_1)G_{C;\gamma\zeta}^R(t_1,t_2)\chi_\zeta(\vec{r}_2)$, and the linear combination of atomic orbital (LCAO) expansion of the molecular orbital: $\varphi_a=\Sigma_\mu C_{\mu,a}^R\chi_\mu$ and $\psi_a=\Sigma_\mu C_{\mu,a}^A\chi_\mu$. Details are described in Appendix A. Because of the non-Hermitian nature of the Hamiltonian $\mathbf{F}+\mathbf{\Sigma}_{contact}^R+\mathbf{\Sigma}_{e\text{-}mv}^R$, the molecular orbital energy ε_a takes a complex value and the molecular orbitals $\{\varphi_a(\vec{r})\}$ and $\{\psi_a(\vec{r})\}$ defined on the dual space are also complex. They are orthonormal to each other: $\int\psi_a(r)\varphi_b^*(r)dr=\delta_{ab}$. One of the authors successfully used this expression to calculate the ballistic-electric current through the benzenedithiolate molecule within the *ab initio* Hartree-Fock nonequilibrium Green's function scheme augmented with a one-dimensional tight-binding model for electrodes.[29] The theory is fully consistent with that given in terms of the inverse of a Hamiltonian-based matrix as it is discussed in Appendix A. The advantage of using the molecular orbital is that it is amenable to simplification. The non-Hermitian effect may be neglected for molecules whose molecular orbital energy is separated by a large gap from the Fermi level of the electrode. We suppose that $\mathbf{\Sigma}_{contact}^R+\mathbf{\Sigma}_{e\text{-}mv}^R$ is less important in the Schrödinger equation than $\mathbf{F}$. Thus, the following Rayleigh-Schrödinger perturbation expansion may be useful:[29,33,34]

$$[\mathbf{F}+\mathbf{\Sigma}_{contact}^R+\mathbf{\Sigma}_{e\text{-}mv}^R](\mathbf{C}_a^{(0)}+\mathbf{C}_a^{R(1)}+\cdots) = (\varepsilon_a^{(0)}+\varepsilon_a^{(1)}+\cdots)\mathbf{S}(\mathbf{C}_a^{(0)}+\mathbf{C}_a^{R(1)}+\cdots), \quad (28)$$

where the superscript (0),(1),… denotes the order of the perturbation expansion; we have dropped the superscript R for the zeroth order coefficient. Within the first order expansion, the retarded and advanced Green's functions may be given by[29,33,34]

$$\mathbf{G}_C^R(E) = \sum_a^M \frac{\mathbf{C}_a^{(0)}\mathbf{C}_a^{(0)T}}{E-\varepsilon_a^{(0)}-\mathrm{Re}\,\varepsilon_a^{(1)}-i\,\mathrm{Im}\,\varepsilon_a^{(1)}}, \quad (29a)$$

$$\mathbf{G}_C^A(E) = \sum_a^M \frac{\mathbf{C}_a^{(0)}\mathbf{C}_a^{(0)T}}{E-\varepsilon_a^{(0)}-\mathrm{Re}\,\varepsilon_a^{(1)}+i\,\mathrm{Im}\,\varepsilon_a^{(1)}}, \quad (29b)$$

where $\mathbf{F}\mathbf{C}_a^{(0)}=\varepsilon_a^{(0)}\mathbf{S}\mathbf{C}_a^{(0)}$, $\mathbf{C}_a^{(0)}=(C_{1,a}^{(0)}\ C_{2,a}^{(0)}\cdots C_{\zeta,a}^{(0)}\cdots C_{M,a}^{(0)})^T$ and $\varepsilon_a^{(1)}=\mathbf{C}_a^{(0)T}(\mathbf{\Sigma}_{contact}^R+\mathbf{\Sigma}_{e\text{-}mv}^R)\mathbf{C}_a^{(0)}$, and M is the number of the molecular orbitals. The expressions in Eqs. (29a) and (29b) do not include the overlap matrix. Details are discussed in Appendix A. Similarly, the lesser and greater Green's functions may be obtained as follows:

$$\mathbf{G}_C^<(E) = i\sum_a^M \frac{f_p(E)\gamma_a^p+f_q(E)\gamma_a^q-i\sigma_{e\text{-}mv,a}^<}{(E-\varepsilon_a^{(0)}-\mathrm{Re}\,\varepsilon_a^{(1)})^2+(\mathrm{Im}\,\varepsilon_a^{(1)})^2}\mathbf{C}_a^{(0)}\mathbf{C}_a^{(0)T}, \quad (30a)$$

$$\mathbf{G}_C^{>}(E) = -i\sum_a^M \frac{[1-f_p(E)]\gamma_a^p + [1-f_q(E)]\gamma_a^q + i\sigma_{e\text{-}mv,a}^{>}}{(E-\varepsilon_a^{(0)} - \mathrm{Re}\,\varepsilon_a^{(1)})^2 + (\mathrm{Im}\,\varepsilon_a^{(1)})^2} \times \mathbf{C}_a^{(0)}\mathbf{C}_a^{(0)T}, \tag{30b}$$

where $\gamma_a^{p(q)} = \mathbf{C}_a^{(0)T}\mathbf{\Gamma}_{p(q)}\mathbf{C}_a^{(0)}$ and $\sigma_{e\text{-}mv,a}^{<(>)} = \mathbf{C}_a^{(0)T}\mathbf{\Sigma}_{e\text{-}mv}^{<(>)}\mathbf{C}_a^{(0)}$. Because $\mathrm{Im}[\mathbf{\Sigma}_{contact}^R(E)] = \boldsymbol{\tau}^T\,\mathrm{Im}[\mathbf{G}_p^R(E) + \mathbf{G}_q^R(E)]\boldsymbol{\tau}$ is given by the electrode state density, it may be small around the molecular orbital energy range when the gap is large. The lowest-order argument discussed above is expected to work well for molecules. The lowest-order calculation result for the benzenedithiolate molecule agreed well with the full calculation made using Eq. (27a). Within the lowest-order scheme, the density matrix may be written as

$$\mathbf{P}(V) = \frac{1}{2\pi i}\int_{-\infty}^{\infty}\mathbf{G}_C^{<}(E)dE = \sum_a n_a(V)\mathbf{C}_a^{(0)}\mathbf{C}_a^{(0)T}, \tag{31a}$$

$$n_a(V) = \frac{1}{2\pi}\int_{-\infty}^{\infty}\frac{f_p(E)\gamma_a^p + f_q(E)\gamma_a^q - i\sigma_{e\text{-}mv,a}^{<}}{(E-\varepsilon_a^{(0)} - \mathrm{Re}\,\varepsilon_a^{(1)})^2 + (\mathrm{Im}\,\varepsilon_a^{(1)})^2}dE. \tag{31b}$$

This calculation is very stable numerically, and free from the numerical fluctuations of the voltage dependence of the ballistic electric current often found in literature concerning the NEGF calculations. In this paper, we neglect $\sigma_{e\text{-}mv,a}^{<}$ in the density matrix calculation, as it has already been explained.

Within the lowest-order expansion, the e-mv self-energies may be given as

$$\mathbf{\Sigma}_{e\text{-}mv,a}^{<(>)}(E) = \sum_a \mathbf{S}\mathbf{C}_a^{(0)}\sigma_{e\text{-}mv,a}^{<(>)}\mathbf{C}_a^{(0)T}\mathbf{S}, \tag{32a}$$

$$\sigma_{e\text{-}mv,a}^{<}(E) = i\sum_s \kappa_a^s\left[\frac{b(\omega_s)\{f_p(E-\omega_s)\gamma_a^p + f_q(E-\omega_s)\gamma_a^q - i\sigma_{e\text{-}mv,a}^{<}(E-\omega_s)\}}{(E-\omega_s-\varepsilon_a^{(0)} - \mathrm{Re}\,\varepsilon_a^{(1)})^2 + (\mathrm{Im}\,\varepsilon_a^{(1)})^2} + \frac{\{b(\omega_s)+1\}\{f_p(E+\omega_s)\gamma_a^p + f_q(E+\omega_s)\gamma_a^q - i\sigma_{e\text{-}mv,a}^{<}(E+\omega_s)\}}{(E+\omega_s-\varepsilon_a^{(0)} - \mathrm{Re}\,\varepsilon_a^{(1)})^2 + (\mathrm{Im}\,\varepsilon_a^{(1)})^2}\right], \tag{32b}$$

$$\sigma_{e\text{-}mv,a}^{>}(E) = -i\sum_s \kappa_a^s\left[\frac{\{b(\omega_s)+1\}\{[1-f_p(E-\omega_s)]\gamma_a^p + [1-f_q(E-\omega_s)]\gamma_a^q + i\sigma_{e\text{-}mv,a}^{>}(E-\omega_s)\}}{(E-\omega_s-\varepsilon_a^{(0)} - \mathrm{Re}\,\varepsilon_a^{(1)})^2 + (\mathrm{Im}\,\varepsilon_a^{(1)})^2} + \frac{b(\omega_s)\{[1-f_p(E+\omega_s)]\gamma_a^p + [1-f_q(E+\omega_s)]\gamma_a^q + i\sigma_{e\text{-}mv,a}^{>}(E+\omega_s)\}}{(E+\omega_s-\varepsilon_a^{(0)} - \mathrm{Re}\,\varepsilon_a^{(1)})^2 + (\mathrm{Im}\,\varepsilon_a^{(1)})^2}\right], \tag{32c}$$

where κ_a^s denotes the e-mv coupling constant between electrons on the molecular orbital a and the normal intramolecular vibration s. Because of the identity relation, $\mathbf{\Sigma}_{e\text{-}mv}^R - \mathbf{\Sigma}_{e\text{-}mv}^A = \mathbf{\Sigma}_{e\text{-}mv}^{>} - \mathbf{\Sigma}_{e\text{-}mv}^{<}$, the imaginary part of the retarded self-energy $\mathrm{Im}(\mathbf{\Sigma}_{e\text{-}mv}^R)$ is given by $\mathrm{Im}(\mathbf{\Sigma}_{e\text{-}mv}^R) = -i/2(\mathbf{\Sigma}_{e\text{-}mv}^{>} - \mathbf{\Sigma}_{e\text{-}mv}^{<})$. Using the Hilbert transform, $\mathbf{\Sigma}_{e\text{-}mv}^R(E) = P/\pi\int \mathrm{Im}(\mathbf{\Sigma}_{e\text{-}mv}^R(E'))/(E-E')dE' + i\cdot\mathrm{Im}(\mathbf{\Sigma}_{e\text{-}mv}^R(E))$, where $P\int_{-\infty}^{\infty}$ denotes the principal value of the integral, we obtain the retarded e-mv self-energy

$$\mathbf{\Sigma}_{e\text{-}mv,a}^R(E) = \sum_a \mathbf{S}\mathbf{C}_a^{(0)}\sigma_{e\text{-}mv,a}^R\mathbf{C}_a^{(0)T}\mathbf{S}, \tag{33a}$$

$$\sigma_{e\text{-}mv,a}^R(E) = \sum_s \kappa_a^s\left[\frac{b(\omega_s)+1}{E-\omega_s-\varepsilon_a^{(0)}-\varepsilon_a^{(1)}} + \frac{b(\omega_s)}{E+\omega_s-\varepsilon_a^{(0)}-\varepsilon_a^{(1)}} - \int\frac{d\omega}{2\pi}\frac{f_p(E-\omega)\gamma_a^p + f_q(E-\omega)\gamma_a^q - i\sigma_{e\text{-}mv,a}^R}{(E-\omega-\varepsilon_a^{(0)} - \mathrm{Re}\,\varepsilon_a^{(1)})^2 + (\mathrm{Im}\,\varepsilon_a^{(1)})^2}\left(\frac{1}{\omega-\omega_s+i\eta} - \frac{1}{\omega+\omega_s+i\eta}\right)\right]. \tag{33b}$$

The squared e-mv coupling constant κ_a^s is diagonal with respect to the molecular orbital suffix a. It is given approximately by

$$\kappa_a^s(V) \cong \frac{1}{2\omega_s(V)}\left[\frac{\partial\varepsilon_a^{(0)}(V)}{\partial q_s}\right]^2, \tag{34}$$

where the normal coordinate gradient of the molecular orbital energy may be given by[35,36]

$$\frac{\partial \varepsilon_a^{(0)}}{\partial q_s} = \sum_{\alpha\beta} \frac{\partial C_{\alpha,a}^{(0)} F_{\alpha\beta} C_{\beta,a}^{(0)}}{\partial q_s}$$
$$= \sum_{\alpha\beta} C_{\alpha,a}^{(0)} C_{\beta,a}^{(0)} \left\{ \frac{\partial H_{\alpha\beta}}{\partial q_s} + \sum_{\gamma\zeta} \left[\frac{\partial P_{\gamma\zeta}(V)}{\partial q_s} \langle \alpha\gamma \| \beta\zeta \rangle + P_{\gamma\zeta}(V) \frac{\partial \langle \alpha\gamma \| \beta\zeta \rangle}{\partial q_s} \right] - \vec{E} \cdot \frac{\partial \langle \alpha | \vec{r} | \beta \rangle}{\partial q_s} - \varepsilon_a^{(0)} \frac{\partial S_{\alpha\beta}}{\partial q_s} \right\}, \tag{35}$$

where q_s is the normal coordinate of the molecular vibration s. $H_{\alpha\beta}=\langle \chi_\alpha(\vec{r})|H|\chi_\beta(\vec{r})\rangle$ and $F_{\alpha\beta}=H_{\alpha\beta}+\Sigma_{\gamma\zeta}P_{\gamma\zeta}\langle\alpha\gamma\|\beta\zeta\rangle - \vec{E}\cdot\langle\alpha|\vec{r}|\beta\rangle$.[28] Details will be discussed in Appendix B.

It might be interesting to discuss the symmetry selection rule on the coupling constant. Because of the group theory, the right-hand side of Eq. (34) takes a nonzero value only for totally symmetric modes,[37,38] while for other modes it vanishes. All the terms in the right-hand side of Eq. (35) are necessary to keep the rule. If some terms, such as the derivative of the overlap matrix or the derivative of the density matrix, are neglected in Eq. (35), we may easily miss important things, and arrive at unexpected results. We should pay special attention to this.

A correction to the zeroth order estimate of the e-mv coupling constant will be discussed. The correction appears because of the contact effect and it will accept lower symmetry contributions. Then we may expect the propensity rule rather than the selection rule at most in our real system. We prefer to use the words "propensity rule" rather than "selection rule" hereafter, because of this.

All the numerical results presented in this paper have been obtained by using the equations given in this section but not using the familiar resolvent calculations. One of the advantages of the lowest-order calculation given here is that it reduces the computational cost because we do not have to take the inverse of the Hamiltonian matrix to calculate the Green's function. Another advantage is the numerical stability in the density matrix calculation and subsequent self-consistent-field calculations.

B. Elastic and inelastic currents

We separated the two self-consistent loops in the numerical calculations, as discussed in Sec. II E. The loop structure adopted in this paper is summarized in Fig. 2. After achieving self-consistency, the electric current is calculated in terms of Eq. (4), using the lesser and greater Green's functions and self-energies. It might be interesting to decompose the total electric current into the following two contributions:

$$I_{elastic,p} = \frac{2e}{h} \int (f_q - f_p) \mathrm{Tr}[\mathbf{G}_C^R \mathbf{\Gamma}_p \mathbf{G}_C^A \mathbf{\Gamma}_q] dE, \tag{36a}$$

$$I_{inelastic,p} = \frac{2e}{h} \int \mathrm{Tr}[\mathbf{\Sigma}_p^{>} \mathbf{G}_C^R \mathbf{\Sigma}_{e\text{-}mv}^{<} \mathbf{G}_C^A - \mathbf{\Sigma}_p^{<} \mathbf{G}_C^R \mathbf{\Sigma}_{e\text{-}mv}^{>} \mathbf{G}_C^A] dE. \tag{36b}$$

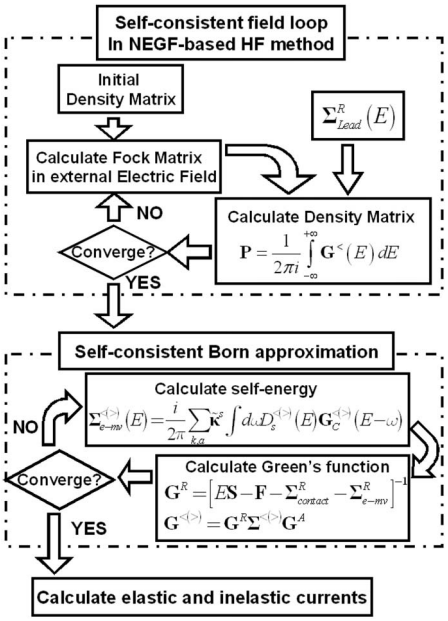

FIG. 2. Self-consistent-field (SCF) loops in NEGF-based Hartree-Fock method and self-consistent Born approximation.

We call the former *elastic* because the formula is analogous to the Landauer form. We designate the remaining latter *inelastic* because the lesser and greater e-mv self-energies appear explicitly in the equation. In the elastic current formula, the retarded and advanced e-mv self-energies are implicitly involved in the retarded and advanced Green's functions, making it different from the ballistic current. The ballistic current is defined by

$$I_{ballistic,p} = \frac{2e}{h} \int (f_q - f_p) \mathrm{Tr}[\mathbf{G}_C^R \mathbf{\Gamma}_p \mathbf{G}_C^A \mathbf{\Gamma}_q] dE, \quad \mathbf{\Sigma}_{e\text{-}mv} = 0. \tag{36c}$$

These definitions will be used in the following section to discuss the numerical calculation results.

IV. CALCULATIONS

A. General details of calculations

We apply the theory discussed hitherto to a hypothetical system where a benzenedithiolate molecule is suspended in the gap between the two electrodes. We adopted standard quantum chemistry techniques to calculate the matrix elements of the center region. A Gaussian basis set is used to expand the Slater-type atomic orbitals whose linear combinations (LCAO) give rise to molecular orbitals. We adopted the STO-6G basis set. While the molecular part is treated in a fully *ab initio* quantum chemistry manner, we used simplifications for the electrodes.[39] The nearest-neighbor approximation is used for τ. We adopted a one-dimensional, single-band tight-binding model (equivalent to a simple Hückel approximation) for the surface density of state, and hence the

surface Green's function of the electrode; $g^R_{surface;p(q)}(E) = \exp(ikc)/\beta$, where kc is obtained by solving $E=\alpha+2\beta\cos(kc)$ for a given E. The parameter values are given by $\alpha=-4.77$ eV and $\beta=-3.0$ eV. The Fermi energy for the model electrodes is set to be $E_F=-4.77$; these parameter values are the same with those used in Ref. 29. The most important thing here is that the energy dependence of the electron density of states (DOS) of the electrode is very gradual. Strong energy dependencies of the DOS give large voltage dependences of the background of the IETS, i.e., d^2I/dV^2. The background may make our discussions on IETS very complicated. We expect this is not the case for the gold electrodes. It should be noted that IETS depends considerably on E_F in the sense that the energy difference between the Fermi energy and the molecular orbital energy is one of the most important parameters which controls the suppression of the elastic current which will be discussed in Sec. IV E. The contact self-energy at the electrode $p(q)$ should be read as

$$\boldsymbol{\Sigma}^R_{p(q)}(E) = \boldsymbol{\tau}^T_{p(q),C} g^R_{surface;p(q)}(E) \boldsymbol{\tau}_{p(q),C} = \begin{pmatrix} t_{p(q),1}t_{p(q),1} & t_{p(q),1}t_{p(q),2} & \cdots & t_{p(q),1}t_{p(q),M} \\ t_{p(q),2}t_{p(q),1} & \ddots & & \vdots \\ \vdots & & \ddots & \vdots \\ t_{p(q),M}t_{p(q),1} & \cdots & \cdots & t_{p(q),M}t_{p(q),M} \end{pmatrix} \times g^R_{surface;p(q)}(E), \quad (37)$$

where $\boldsymbol{\tau}_{p(q),C}=(t_{p(q),1}\ t_{p(q),2}\cdots t_{p(q),\zeta}\cdots t_{p(q),M})$. We further supposed that $t_{p(q),\alpha}=0.0$ for all atomic orbitals χ_α, except the 3py orbital (π type) of the sulfur atom of the p-benzenedithioone diradical molecule. $t_{p(q),\text{3py of sulfur}}=-1.0$ eV.[29] All calculations are done at the ground state ($T=0$ K). It should be noted that our interest here is to clarify the physical effect of the bias voltage on the inelastic electric current problem, rather than to visit every chemical detail of the benzenedithiolate molecule. The simplifications adopted should not affect the understanding of the physics involved in the problem. The simplifications have practical benefits, for instance, the self-consistent calculations for $\boldsymbol{\Sigma}^{R(A)}_{HF}$ and $\boldsymbol{\Sigma}^{>(<)}_{e\text{-}mv}(E)$ are free of instabilities due to inaccurate modeling of the electrodes, such as the effects of finite size on the lateral degrees of freedom, often found in the literature.

B. Electron-intramolecular vibration coupling constant

The normal mode vectors and frequencies are obtained by diagonalizing the NEGF-based Hessian matrix, which is evaluated after the self-consistency of the NEGF is achieved at every value of V sampled. Rather than the squared e-mv coupling constant, κ, the following dimensionless coupling constant, derived from κ, is sometimes seen in physics literature:[40–46]

$$\lambda^s_a = \int_{\mu_p}^{\mu_q} \frac{dE}{eV_{bias}} \mathrm{DOS}(E) \frac{\kappa^s_a}{\hbar\omega_s}. \quad (38)$$

Sergueev *et al.* studied the dimensionless coupling constant

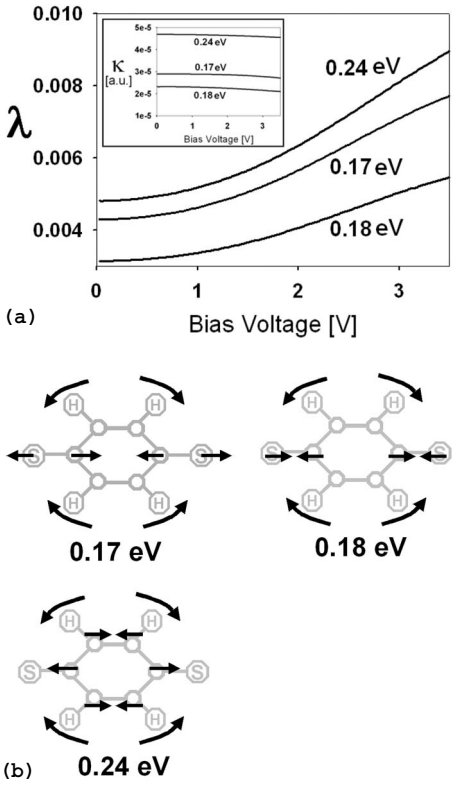

FIG. 3. (a) The dimensionless coupling constant λ as a function of bias voltage. λ increases as the bias voltage increases. The inset shows the voltage dependency of the squared e-mv coupling constant κ. κ does not show clear bias voltage dependency. The numbers marked near the plots denote the energy of the corresponding molecular vibrations. (b) Normal vibrational modes of the benzenedithiolate molecule, which take finite values of the electron-intramolecular vibration (e-mv) coupling constants. The normal modes shown here as examples are calculated at $V_{bias}=0.1$ V.

λ (Ref. 14) and found a very strong bias voltage dependence, which might be suggestive of anomalous inelastic current behavior. Before we discuss the finite bias voltage effect on both the elastic and inelastic currents, we first compare our calculations of the dimensionless coupling constant with those obtained by previous authors. λ^s_a is calculated only for the purpose to compare our results with the preceding ones. κ^s_a given by Eq. (34) is used throughout the paper except this subsection. Our results are shown in Fig. 3(a). Also shown in the inset of the figure is the voltage dependence of the squared e-mv coupling constant $\kappa^s_a(V)$. The bias voltage dependences of the dimensionless coupling constant λ for some vibrational modes obtained in our calculations are qualitatively in fair agreement with those obtained by previous authors.[14] They increase when the voltage becomes larger than 1–2 V. It is clear from the figure, and its inset, that the bias voltage effect on λ comes mostly from the density of state part [DOS(E)]. The bias voltage dependencies of the squared coupling constant $\kappa^s_a(V)$ and vibrational frequencies are very weak. Figure 3(b) shows three normal vibrational modes of the benzenedithiolate molecule. The three totally symmetric modes of the extended molecule in the C_{2v} configuration have significant contributions to e-mv coupling.

C. Equilibrium Green's function and non-equilibrium Green's function calculations

In Sec. II, we discussed the elastic and inelastic e-mv coupling effects on the electric current, based on the non-equilibrium Green's function method, where electron-electron interaction is considered within the Hartree-Fock approximation. The bias voltage-dependent density matrix is accompanied by rearrangement of electron charge distribution in the center region. It is also closely related to charge transfer between the electrode and the molecule, which may result in a change of the total molecular charge. It may be interesting to freeze the rearrangement for clear understanding. This may be achieved by keeping the occupation number of the molecular orbitals independent of V; that is, we freeze $\mathbf{F}$ to the value obtained when $V=0$. The bias voltage dependence of the electric current is calculated using this $\mathbf{F}$ within the linear response scheme. This is analogous to the tight-binding calculation, but the mean-field potential, which is decided at $V=0$, is now included. We call this method the equilibrium Green's function (EGF) method[17,29] as opposed to the full calculations based on the nonequilibrium Green' function (NEGF) method. In this method, no self-consistent calculation is made for the electron-electron interaction, except at $V=0$, and we assume $\mathbf{\Sigma}_{HF}^{R(A)}(V\neq 0)=\mathbf{\Sigma}_{HF}^{R(A)}(V=0)$. We use the notations NEGF and EGF to specify whether self-consistent calculation for the electron-electron interaction for every V, including $V\neq 0$, is made before the self-consistent Born calculation for e-mv coupling or not. This procedure is applied to EGF calculations of the e-mv coupling constants and the normal molecular vibrations as well.

It should be emphasized that EGF calculation results will be presented here just as references to exaggerate how the bias voltage and the electron-electron interaction affect the NEGF results of the vibronic current. Because of this, we have frozen all the bias voltage-dependent changes of the electronic structure of the center region in the EGF calculations including the field gradient and the charge-transfer contributions to the changes. It should be noted that the charge-transfer effect has much larger contributions to the energy level shift than the field gradient effect in the NEGF calculations of the benzenedithiolate molecule.

D. Elastic and inelastic currents in the low-bias voltage region

We discuss here the elastic and inelastic currents in the low-bias region. The total current is given by a sum of elastic and inelastic currents. We calculated these currents based on both EGF and NEGF methods and summarized our results in Fig. 4. The bias voltage dependence of the differential conductance dI/dV's obtained using both EGF and NEGF methods are shown in Fig. 4(a). The corresponding counterparts for d^2I/dV^2 obtained using both methods are shown in Fig. 4(b). All intramolecular vibrational modes are considered simultaneously in the calculations. We find three steps of the differential conductance, dI/dV, at V=0.17, 0.18, and 0.24 V in both EGF and NEGF results, shown in Fig. 4(a). These peaks come from e-mv coupling to the three normal vibrational modes, given in Fig. 3(b). The magnitudes of the gaps at every step are comparable between the EGF and the NEGF results, but the dI/dV value itself is found to be larger in the EGF results than in the NEGF results. The difference is mostly determined at a bias voltage region smaller than the first step. The finite value of the differential conductance dI/dV at $V=0$ appears because of the small tails of the electrodes' electronic density of state. However, we cannot find a clear difference between d^2I/dV^2's obtained by the EGF and NEGF methods, as shown in Fig. 4(b). The two plots for d^2I/dV^2, given in Fig. 4(b), coincide and seem to merge into a single curve, other than some small fluctuations due to the finite-difference methods used in the calculations. The peaks of d^2I/dV^2 appear at the same voltage as the steps of dI/dV, i.e., at $V=0.17$, 0.18, and 0.24 V. These peaks correspond to the totally symmetric modes of the benzenedithiolate molecule, whose symmetry is reduced to C_{2v}, because of the presence of the external electronic field along the molecular axis. There is virtually no difference between the EGF and NEGF results because the molecular vibration frequencies $\omega_s(V)$ and the squared coupling constants $\kappa_a^s(V)$ do not depend much on applied bias voltages. The finite bias effect does not play an important role in the low-bias region, where experimental measurements of IETS are often made.

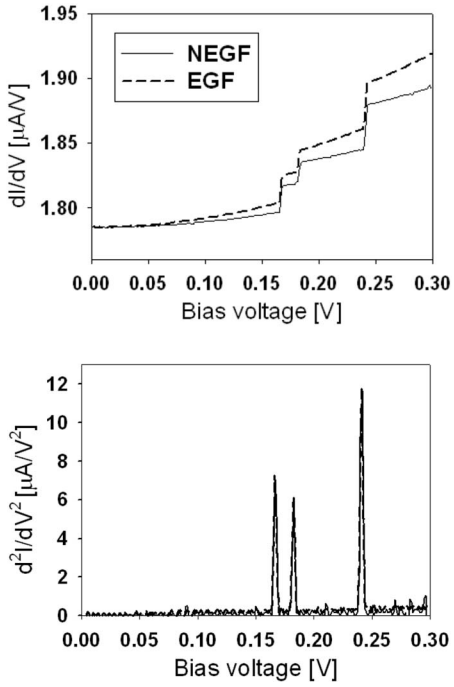

FIG. 4. (a) dI/dV and (b) d^2I/dV^2 curves. The solid and dashed lines denote the NEGF and the EGF calculation results, respectively.

E. Elastic and inelastic currents in the high-bias voltage region

Here, we discuss the calculation results in the high-bias region. The calculation results of the I-V curves obtained using the EGF and NEGF methods are summarized in Fig. 5. The EGF results are shown in Fig. 5(a), and the NEGF results are shown in Fig. 5(b). The total electric currents are plotted in both figures, as well as their decomposition into

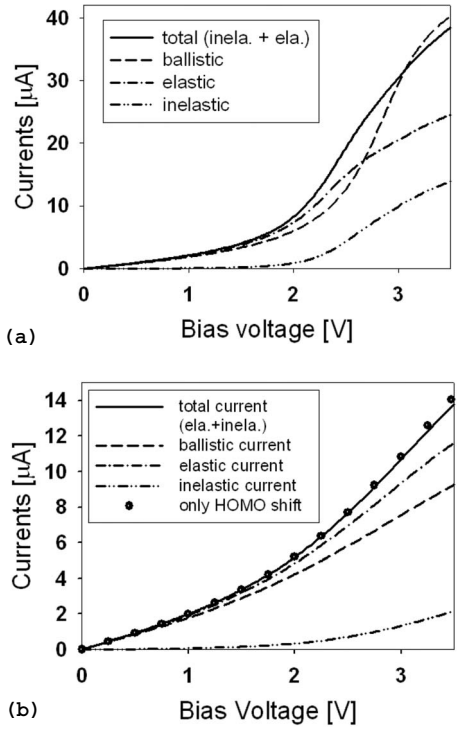

FIG. 5. Current vs voltage plots, denoted from (a) the EGF and (b) the NEGF calculation results. The solid lines denote the total current, which is given as the sum of the elastic and the inelastic currents. The dashed lines denote the ballistic current. The dotted and the double-dotted lines represent the elastic and inelastic currents, respectively. The filled circles are obtained from the EGF calculation supplemented by the HOMO energy shift whose value is estimated from the NEGF calculation results.

elastic and inelastic contributions. Also plotted as references are the ballistic currents calculated using the two methods. The EGF calculation results are discussed first. We find in Fig. 5(a) that while the inelastic current increases as the voltage increases, the total current is suppressed in the high-bias region compared with the ballistic current. This is because the retarded e-mv self-energy increases as the bias voltage exceeds 2 V. The increase results in the suppression of the retarded Green's functions, which leads to the suppression of the elastic current. The total current is reduced because the decrease in the elastic channel is larger than the increase in the inelastic channel. In this case, an increase of the e-mv self-energy enhances the inelastic channel, but works to suppress the elastic channel to a greater degree, resulting in the reduction of the total current. It should be noted that the bias voltage range where the suppressive correlation between the elastic and the inelastic channels appears depends on the energy difference between the molecular orbital energy and the Fermi energy of electrodes.

Next, we discuss the NEGF calculation results, where the results are quite the opposite. We do not observe suppression of the total and elastic currents at high-bias voltage at all in Fig. 5(b). Note that the magnitudes of the electric currents obtained by the NEGF method are several times smaller than those of the EGF. This may come from the energy level shift due to the voltage, which is considered only in the NEGF calculation, through the change of the molecular charge. The correlation between the elastic and inelastic channels is found to be overestimated when we do not consider the charge of self-consistency between the molecule and the electrodes. It is therefore very important to consider this effect before we discuss the vibronic corrections made to the electric current in the high-bias voltage region. The differences between the NEGF and the EGF results involve some important information on the vital role played by bias voltage and the electron-electron interaction in the vibronic current at high-bias voltage. They will be discussed in Sec. V B.

V. DISCUSSIONS

A. Small gap cases

When the gap is small, we might have to include the higher-order correction terms of the Rayleigh-Schrödinger expansion, given by Eq. (28). The leading correction term to the e-mv coupling constant may be given by $\kappa_a^{s,(1)}=(1/2\omega_s)\times(\partial[\mathbf{C}_a^{(0)T}(\mathbf{\Sigma}_{contact}^R)\mathbf{C}_a^{(0)}]/\partial q_s)^2$. The correction term may accept lower symmetry contributions. This lowest-order correction may be involved in the e-mv coupling constant, which may play a similar role as the scattering state effect discussed in Ref. 14. In both cases, the coupling constants are not real, but complex. This is a serious problem for the theory. Even worse, because the inelastic current is dependent on the electronic local density of state, the vibrational local density of state, and the coupling constant, competitions and correlations among them make the arguments on vibration mode dependence very complicated in the small gap region. To make a clear assignment of the mode dependence, both theoretically[47–50] and experimentally,[51,52] the large gap region is the place to start the discussion. Here the electronic density of state of the electrodes may not play an important role, because the density of state may fall off rapidly in the important energy region. When the gap is large, $\varepsilon_a^{(0)}$ is a very good estimate of the molecular orbital energy, hence the e-mv coupling constant given by Eq. (34) should work well.

It should be pointed out here that a unique calculation given by Troisi and Ratner may include contact effects on the e-mv coupling constant to some extent effectively.[47] It is, however, quite difficult to find any correspondence of their Taylor expansion in our Keldysh Green's function theory. Quantitative comparison between our theory and their theory is hence difficult to make.

B. Charge-transfer effect

In the NEGF method, the molecule is allowed to respond to bias voltages by changing the occupation numbers, hence the density matrix. The molecule is allowed to change the molecular charge. In the case of benzenedithiolate molecule, a hole transfers from electrodes to the molecule that destabilizes the molecule and pushes the HOMO energy down to accept the incoming electrons as seen in Fig. 6. The total number of electrons in the molecule is reduced as we increase the voltage, as shown in the inset of Fig. 6. The energy shift may be confirmed from another figure, which

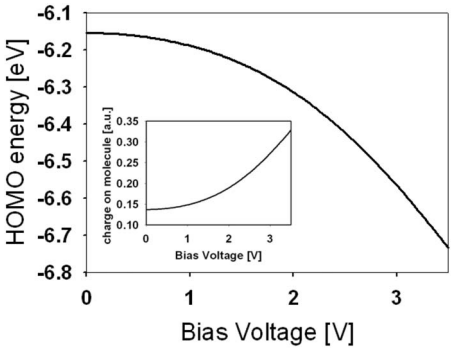

FIG. 6. The HOMO energy shift according to the applied bias voltages. The voltage dependence of the total charge in the benzenedithiolate molecule is shown in the inset. The HOMO energy is pushed down as the voltage increases, which increases the total charge on the molecule. The total charge is defined by $-\Sigma_r 2P_{rr} + \Sigma_A Z_A$.

shows the voltage dependence of the energy-dependent transmission probability. The peak of transmission probability for ballistic current, shown in Fig. 7, shifts down as the voltage increases. Because of the shift, the suppression at high-bias voltage, found in the EGF result, is not found in the NEGF result. The suppression, and hence the increase of the e-mv self-energy, appear in the EGF result because the chemical potential of the electrode p is reduced as we increase the bias voltage, to fall close to the HOMO energy. This does not appear in the NEGF result since the gap between the chemical potential and the molecular orbital energy is not filled because of the reduction of the HOMO energy. The energy and the potential do not come near each other within the voltage region studied. In fact, the total electric current obtained using the NEGF method can be simulated by the EGF calculation if we consider the HOMO shift as demonstrated by the circle in Fig. 5(b). While the charge transfer modulates both spatial expansions of molecular orbitals and the molecular orbital energy level structure, Fig. 5(b) shows that the latter is more important to reduce the suppressive correlation. The shift of molecular orbitals works as if it screens the bias voltage effect. For example, electric

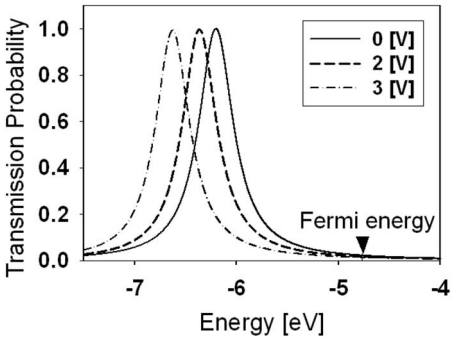

FIG. 7. Transmission probability of the HOMO. The peak of transmission probability shifts down as we increase bias voltage. The solid, dashed, and dotted lines denote the transmission probabilities at 0, 2, and 3 V, respectively.

current behavior around 3 V in the NEGF result seems similar to that obtained at about 2 V using the EGF method. It should be noted that the NEGF method, in principle, may not exclude the suppressive correlation between the elastic and inelastic components of the current in the higher-bias voltage region than studied here. It may appear sooner or later at higher-bias voltage because the rate of the HOMO energy shift is expected to be different from that of the chemical potential, in general.

The bias voltage effect is found to play an important role in the high-bias voltage region. The energy shift accompanying the small change of the molecular charge, which is considered appropriately only when the NEGF SCF loop is fully solved, plays a very important role in correcting the overestimation of the suppressive correlation between the inelastic and elastic channels. Similar behavior to that of the EGF results for the high-bias voltage region has been observed in the resonant case, namely, atomic wires. When the gap is small, the elastic and total currents decrease when the bias voltage exceeds the phonon energy, while the inelastic current increases as the bias voltage exceeds the phonon energy. Then the peak and dip structure in the resonant region, as a function of the bias voltage, behaves quite oppositely from the tunneling region.[53] Because a charge transfer between the molecule and the electrodes is not expected in the zero-gap case, it may not be likely that the charge transfer modifies the zero-gap results much. However, when the gap is marginal, it may be interesting to determine if the change in charge reduces the suppressive correlation between the elastic and inelastic channels. The model adopted here for the electrodes is not capable of including details of the interactions between the molecule and the electrodes in the resonant case. It may be far too simplified to address the problem. The problem in the resonant regime remains an open question.

VI. CONCLUSIONS

We have studied the bias voltage dependence of the elastic and inelastic currents of the e-mv origin in the tunneling region, where the gap between E_F and the site energy is larger, compared with twice of the intramolecular transfer integral. Two self-consistent loops, one treat the electron-electron interaction within the Hartree-Fock approximation and another to treat e-mv coupling within the Born approximation, are derived and solved. It was found that the bias voltage effect does not produce an essential change in the elastic and inelastic currents in the low-bias voltage region. In the experimentally accessible voltage region, however, the bias voltage effect on the vibronic current problem is expected to be very small. A small change of the molecular charge, induced by a high-bias voltage, however, reduces the suppressive correlation between the elastic and inelastic channels. In the high-bias voltage region, the e-mv coupling effect on the current is strongly modified by the voltage.

APPENDIX A: MATRIX REPRESENTATIONS OF THE GREEN'S FUNCTION

Here we discuss two matrix representations of the retarded Green's function based on atomic orbital (AO). One is

given in terms of the Lehmann representation and the other in terms of the inverse of a Hamiltonian-based matrix. The former is given by

$$G_C^R(\vec{r}_1,\vec{r}_2;E) = \sum_a^M \frac{\varphi_a(\vec{r}_1)\psi_a^*(\vec{r}_2)}{E-\varepsilon_a}. \tag{A1}$$

The retarded Green's function satisfies the following equation:

$$[E+i\eta-F(\vec{r}_1)]G_C^R(\vec{r}_1,\vec{r}_2;E) - \int d\vec{r}[\Sigma_{contact}^R(\vec{r}_1,\vec{r}_3) + \Sigma_{e\text{-}mv}^R(\vec{r}_1,\vec{r}_3)]G_C^R(\vec{r}_3,\vec{r}_2;E) = \delta(\vec{r}_1-\vec{r}_2), \tag{A2}$$

which is equivalent to Eq. (2a). After making the LCAO expansion of the molecular orbitals $\{\varphi_a\}$ and $\{\psi_a\}$ involved in G_C^R, we multiply $\chi_\mu(\vec{r}_1)$ from the left-hand side and $\chi_\zeta(\vec{r}_2)$ from the right to Eq. (A2), then take the integrals over $\vec{r}_1$ and $\vec{r}_2$ as follows:

$$\begin{aligned}
&\sum_a\sum_{\nu,\gamma}\int \chi_\mu(\vec{r}_1)[E+i\eta-F(\vec{r}_1)]\chi_\nu(\vec{r}_1)d\vec{r}_1 \\
&\quad\times\frac{C_{\nu,a}^R C_{\gamma,a}^{A*}}{E-\varepsilon_a+i\eta}\int \chi_\gamma(\vec{r}_2)\chi_\zeta(\vec{r}_2)d\vec{r}_2 + \int\int \chi_\mu(\vec{r}_1) \\
&\quad\times[\Sigma_{contact}^R(\vec{r}_1,\vec{r}_3)+\Sigma_{e\text{-}mv}^R(\vec{r}_1,\vec{r}_3)]\chi_\nu(\vec{r}_3)d\vec{r}_1 d\vec{r}_3 \\
&\quad\times\sum_a\frac{C_{\nu,a}^R C_{\gamma,a}^{A*}}{E-\varepsilon_a+i\eta}\int \chi_\gamma(\vec{r}_2)\chi_\zeta(\vec{r}_2)d\vec{r} \\
&\quad=\int\int \chi_\mu(\vec{r}_1)\delta(\vec{r}_1-\vec{r}_2)\chi_\zeta(\vec{r}_2)d\vec{r}_1 d\vec{r}_2.
\end{aligned} \tag{A3}$$

Thus we obtain

$$\sum_{\nu,\gamma}[(E+i\eta)S_{\mu\nu}-F_{\mu\nu}-\Sigma_{contact;\mu\nu}^R - \Sigma_{e\text{-}mv;\mu\nu}^R]\sum_a\frac{C_{\nu,a}^R C_{\gamma,a}^{A*}}{E-\varepsilon_a+i\eta}S_{\gamma\zeta} = S_{\mu\zeta}. \tag{A4}$$

Multiplying $\mathbf{S}^{-1}$ from the right, we obtain the equation

$$[(E+i\eta)\mathbf{S}-\mathbf{F}-\mathbf{\Sigma}_{contact}^R-\mathbf{\Sigma}_{e\text{-}mv}^R]\mathbf{G}_C^R = \mathbf{I}. \tag{A5}$$

Because the retarded Green's function given by Eq. (A1) satisfies Eq. (A5), Green's function, given in terms of the Lehmann representation, is equivalent to that given by the inverse.

APPENDIX B: ELECTRON-INTRAMOLECULAR VIBRATION COUPLING CONSTANT AND THE GRADIENT OF THE MOLECULAR ORBITAL ENERGY

In this appendix, we derive Eqs. (34) and (35). We denote the following one-body Hamiltonian:

$$\hat{F}_0 = \sum_a \varepsilon_a^{(0)}\hat{c}_a^\dagger\hat{c}_a, \tag{B1}$$

where $\hat{c}_a^\dagger$ is the creation operator of an electron on the molecular orbital a. Within the linear expansion of $\varepsilon_a^{(0)}$, in terms of the normal coordinate, the one-body Hamiltonian may be expressed by $\hat{F}=\hat{F}_0+\hat{F}_{e\text{-}mv}$, where $\hat{F}_{e\text{-}mv}=\Sigma_k\Sigma_a(\partial\varepsilon_a^{(0)}/\partial q_k)\hat{c}_a^\dagger\hat{c}_a q_k$. If we use creation and annihilation operators for molecular vibration, $\hat{b}_k^\dagger$ and $\hat{b}_k$, noting $q_k=(\hat{b}_k^\dagger+\hat{b}_k)/\sqrt{2\omega_k}$, then we have

$$\hat{F}_{e\text{-}mv} = \sum_k\sum_a\frac{1}{\sqrt{2\omega_k}}\frac{\partial\varepsilon_a^{(0)}}{\partial q_k}\hat{c}_a^\dagger\hat{c}_a(\hat{b}_k^\dagger+\hat{b}_k). \tag{B2}$$

Because the lowest self-energy due to the e-mv coupling has two vertices, the e-mv coupling constant κ given by Eq. (20) in the molecular orbital representation may be written as the square of the coefficient $(1/\sqrt{2\omega_k})(\partial\varepsilon_a^{(0)}/\partial q_k)$, which is equivalent to Eq. (34). The gradient of molecular orbital energy is given as

$$\begin{aligned}
\frac{\partial}{\partial q_k}\varepsilon_a^{(0)} &= \frac{\partial}{\partial q_k}\sum_{\alpha,\beta}C_{\alpha,a}^{(0)}C_{\beta,a}^{(0)}F_{\alpha\beta} \\
&= \sum_{\alpha,\beta}\left\{C_{\alpha,a}^{(0)}C_{\beta,a}^{(0)}\frac{\partial F_{\alpha\beta}}{\partial q_k} + F_{\alpha\beta}\left(\frac{\partial C_{\alpha,a}^{(0)}}{\partial q_k}C_{\beta,a}^{(0)} + C_{\alpha,a}^{(0)}\frac{\partial C_{\beta,a}^{(0)}}{\partial q_k}\right)\right\} \\
&= \sum_{\alpha,\beta}\left\{C_{\alpha,a}^{(0)}C_{\beta,a}^{(0)}\frac{\partial F_{\alpha\beta}}{\partial q_k} + \varepsilon_a^{(0)}S_{\alpha\beta}\left(\frac{\partial C_{\alpha,a}^{(0)}}{\partial q_k}C_{\beta,a}^{(0)} + C_{\alpha,a}^{(0)}\frac{\partial C_{\beta,a}^{(0)}}{\partial q_k}\right)\right\}.
\end{aligned} \tag{B3}$$

If we notice the following relation:

$$\sum_{\alpha,\beta}\left\{\frac{\partial C_{\alpha,a}^{(0)}}{\partial q_k}S_{\alpha\beta}C_{\beta,a}^{(0)} + C_{\alpha,a}^{(0)}\frac{\partial S_{\alpha\beta}}{\partial q_k}C_{\beta,a}^{(0)} + C_{\alpha,a}^{(0)}S_{\alpha\beta}\frac{\partial C_{\beta,a}^{(0)}}{\partial q_k}\right\} = 0, \tag{B4}$$

which is derived from the normal condition for the molecular orbital, $\Sigma_{\alpha,\beta}C_{\alpha,a}^{(0)}S_{\alpha\beta}C_{\beta,a}^{(0)}=1$, we obtain Eq. (35).

[1] G. Guniberti, G. Fagas, and K. Richter, *Introducing Molecular Electronics* (Springer-Verlag, Berlin, 2005).

[2] A. S. Alexandrov, J. Demsar, and E. I. K. Yanson, *Molecular Nanowires and Other Quantum Objects* (Kluwer, Dordrecht, 2004).

[3] S. N. Yaliraki, A. E. Roitberg, C. Gonzalez, V. Mujica, and M. A. Ratner, J. Chem. Phys. **111**, 6997 (1999).

[4] A. Nitzan, *Chemical Dynamics in Condensed Phases* (Oxford University Press, New York, 2006).

[5] V. Mujica, M. Kemp, and M. A. Ratner, J. Chem. Phys. **101**,

6856 (1994).
[6] Y. Asai and H. Fukuyama, Phys. Rev. B **72**, 085431 (2005).
[7] T. Frederiksen, M. Brandbyge, N. Lorente, and A. P. Jauho, Phys. Rev. Lett. **93**, 256601 (2004).
[8] Y. Asai, Phys. Rev. Lett. **93**, 246102 (2004); **94**, 099901(E) (2005).
[9] Y.-C. Chen, M. Zwolak, and M. Di Ventra, Nano Lett. **4**, 1709 (2004).
[10] Y. Asai and T. Shimazaki, *Charge Migration in DNA; Physics, Chemistry and Biology Perspectives* (Springer-Verlag, Berlin, 2007).
[11] W. Ho, J. Chem. Phys. **117**, 11033 (2002).
[12] N. Agraït, C. Untiedt, G. Rubio-Bollinger, and S. Vieira, Phys. Rev. Lett. **88**, 216803 (2002).
[13] J. K. Viljas, J. C. Cuevas, F. Pauly, and M. Hafner, Phys. Rev. B **72**, 245415 (2005).
[14] N. Sergueev, D. Roubtsov, and H. Guo, Phys. Rev. Lett. **95**, 146803 (2005).
[15] J. Taylor, H. Guo, and J. Wang, Phys. Rev. B **63**, 121104(R) (2001).
[16] M. Brandbyge, J.-L. Mozos, P. Ordejon, J. Taylor, and K. Stokbro, Phys. Rev. B **65**, 165401 (2002).
[17] Y. Xue, S. Datta, and M. A. Ratner, Chem. Phys. **281**, 151 (2002).
[18] Y. Xue and M. A. Ratner, Phys. Rev. B **68**, 115406 (2003).
[19] T. Rakshit, G.-C. Liang, A. W. Ghosh, M. Hersam, and S. Datta, Phys. Rev. B **72**, 125305 (2005).
[20] T. Shimazaki and K. Yamashita, Nanotechnology **18**, 424012 (2007).
[21] Y.-C. Chen, M. Zwolak, and M. Di Ventra, Nano Lett. **3**, 1691 (2003).
[22] G. D. Mahan, *Many-Particle Physics*, 3rd ed. (Kluwer, Dordrecht/Plenum, New York, 2000).
[23] S. Datta, *Electronic Transport in Mesoscopic Systems* (Cambridge University Press, Cambridge, 1995).
[24] L. P. Kadanoff and G. Baym, *Quantum Statistical Mechanics* (Benjamin, London, 1962).
[25] J. Taylor, M. Brandbyge, and K. Stokbro, Phys. Rev. B **68**, 121101(R) (2003).
[26] A. L. Fetter and J. D. Walecka, *Quantum Theory of Many-Particle Systems* (Dover, Mineola, TX, 2003).
[27] M. Galperin and A. Nitzan, Ann. N.Y. Acad. Sci. **1006**, 48 (2003).
[28] F. Jensen, *Introduction to Computational Chemistry* (Wiley, Chichester, 1999).
[29] T. Shimazaki, Y. Xue, M. A. Ratner, and K. Yamashita, J. Chem. Phys. **124**, 114708 (2006).
[30] T. N. Todorov, J. Hoekstra, and A. P. Sutton, Philos. Mag. B **80**, 421 (2000).
[31] M. Di Ventra, Y.-C. Chen, and T. N. Todorov, Phys. Rev. Lett. **92**, 176803 (2004).
[32] D. C. Langreth, *Linear and Nonlinear Electron Transport in Solids* (Plenum, New York, 1976).
[33] T. Shimazaki, H. Maruyama, Y. Asai, and K. Yamashita, J. Chem. Phys. **123**, 164111 (2005).
[34] H. Nakamura and K. Yamashita, J. Chem. Phys. **124**, 194106 (2006).
[35] J. Gerratt and I. M. Mills, J. Chem. Phys. **49**, 1719 (1968).
[36] J. A. Pople, R. Krishnan, H. B. Schlegel, and J. S. Binkley, Int. J. Quantum Chem., Quantum Chem. Symp. **13**, 225 (1979).
[37] F. A. Cotton, *Chemical Application of Group Theory*, 2nd ed. (Wiley, New York, 1971).
[38] N. O. Lipari, M. J. Rice, C. B. Duke, R. Bozio, A. Girlando, and C. Pecile, Int. J. Quantum Chem., Quantum Chem. Symp. **11**, 583 (1977).
[39] W. Tian, S. Datta, S. Hong, R. Reifenberger, J. I. Henderson, and C. P. Kubiak, J. Chem. Phys. **109**, 2874 (1998).
[40] T. Ishiguro and K. Yamaji, *Organic Superconductors* (Springer-Verlag, Tokyo, 1989).
[41] Y. Asai, Phys. Rev. B **68**, 014513 (2003).
[42] Y. Asai, Phys. Rev. B **49**, 4289 (1994).
[43] Y. Asai and Y. Kawaguchi, Phys. Rev. B **46**, 1265 (1992).
[44] O. Gunnarsson, Rev. Mod. Phys. **69**, 575 (1997).
[45] M. S. Dresselhaus, G. Dresselhaus, and P. C. Eklund, *Science of Fullerenes and Carbon Nanotubes* (Academic, New York, 1996).
[46] W. E. Picket, *Solid State Physics* (Academic, New York, 1994).
[47] A. Troisi and M. A. Ratner, Phys. Rev. B **72**, 033408 (2005).
[48] J. Jiang, M. Kula, W. Lu, and Y. Luo, Nano Lett. **5**, 1551 (2005).
[49] M. Paulsson, T. Frederiksen, and M. Brandbyge, Nano Lett. **6**, 258 (2006).
[50] J. B. Maddox, U. Harbola, N. Liu, L. Silien, W. Ho, G. C. Bazan, and S. Mukamel, J. Phys. Chem. A **110**, 6329 (2006).
[51] J. G. Kushmerick, J. Lazorcik, C. H. Patterson, R. Shashidhar, D. S. Seferos, and G. C. Bazan, Nano Lett. **4**, 639 (2004).
[52] W. Wang, T. Lee, I. Kretzschmar, and M. A. Reed, Nano Lett. **4**, 643 (2004).
[53] M. Galperin, M. A. Ratner, and A. Nitzan, J. Chem. Phys. **121**, 11965 (2004).